

Clinical evaluation of the respiratory mechanics using accelerated 3D dynamic free breathing MRI reconstruction

Sampada Bhavé¹, Sajan Goud Lingala², Scott Nagle³, John D Newell Jr⁴, and Mathews Jacob¹

¹Electrical and Computer Engineering, University of Iowa, Iowa City, IA, United States, ²Electrical Engineering, University of Southern California, Los Angeles, CA, United States, ³Radiology, University of Wisconsin School of Medicine and Public Health, Madison, WI, United States, ⁴Radiology, University of Iowa, Iowa City, IA, United States

Synopsis

Three-dimensional dynamic MRI (3D-DMRI) is a promising method to analyze respiratory mechanics. However, current 3D DMRI implementations offer limited temporal, spatial resolution and volume coverage. In this work we demonstrate the feasibility of three compressed sensing reconstruction methods along with view-sharing method with clinical evaluation on 8 healthy subjects by expert radiologists. BCS scheme provides better performance than other schemes both qualitatively and quantitatively. The preliminary results on lung volume changes demonstrate the clinical utility of the BCS scheme.

Introduction:

Dynamic imaging of respiratory mechanics play an important role in the diagnosis of the abnormalities involved in respiratory pumping, including diaphragm paresis or paralysis and abnormal chest wall mechanics resulting from neuromuscular, pulmonary, or obesity related disorders^{1,2}. Current standard of care techniques like spirometry, plethysmography detects global changes, which occur during the advanced stages of the disease. While 2D imaging techniques can offer high temporal resolution, it is challenging to merge the information from multiple 2D slices for the 3D visualization of the diaphragmatic dome and volume measurements because of the irregular nature of respiratory motion. In this work, we evaluate the feasibility of three compressed sensing schemes, namely nuclear norm minimization based low-rank scheme, ℓ_1 Fourier sparsity regularization scheme, blind compressed sensing (BCS)^{3,4}, and the commonly used view-sharing scheme to enable the imaging of respiratory dynamics with full coverage of the thorax and improved spatial and temporal resolution needed to image tidal breathing. Two expert radiologists quantitatively scored the reconstructions on a four-point scale to assess diagnostic image quality.

Methods:

8 healthy volunteers (5 males and 3 females; median age: 28) without any evidence of pulmonary disease were scanned on the Siemens 3T Trio scanner (Siemens AG, Healthcare sector, Erlangen, Germany) with a 32-channel body array coil. The prospectively undersampled 3D dynamic data was collected using a FLASH sequence with a golden angle radial 3D stack of stars trajectory. The sequence parameters are: FOV= 350x350mm², TR/TE= 2.37ms/0.92ms, P/F: 6/8, matrix: 128x128, and spatial resolution: 2.7x2.7x10mm³. 16 slices with 3500 spokes per slice we acquired to obtain whole lung coverage. The data was binned by considering 16 radial spokes per frame resulting in a temporal resolution of 495ms/frame. Two datasets were collected from the 8th subject, one while free breathing and one while breathing from functional residual capacity (FRC) to total lung capacity (TLC) to demonstrate the feasibility of BCS scheme with different maneuvers. These datasets were reconstructed using the nuclear norm minimization scheme, ℓ_1 Fourier sparsity regularization scheme, BCS scheme and the view-sharing scheme, which differ in the way they model the temporal profiles of the dynamic data. The nuclear norm minimization scheme assumes the temporal profiles to be low-rank while the ℓ_1 Fourier sparsity regularization scheme exploits the sparsity of the data in the Fourier domain along the temporal dimension (x-f space) assuming that respiratory motion is pseudo-periodic in nature. The BCS scheme models the temporal profiles as a sparse linear combination of atoms from a learned dictionary as in^{3,4}. Each of the 3D reconstructions was

evaluated for spatial resolution, temporal resolution and artifacts by two expert cardiothoracic radiologists (R1 and R2) using a four-point scale (4-Outstanding Diagnostic Quality, 3- Good Diagnostic Quality, 2- Average Diagnostic Quality, 1- Limited Diagnostic Quality and 0- un-interpretable). To demonstrate the potential applications of this work, the lung was segmented using a region-growing algorithm after reconstruction. The lung volume was calculated in terms of the number of pixels within the lung region.

Results:

Table 1 shows the visual scores of all the four methods by both the radiologists (denoted as R1 and R2) based on three factors: 1.a – Aliasing artifacts, 1.b – Temporal blurring and 1.c – Spatial blurring. The scores suggest that the BCS scheme performs better than other schemes in the temporal blurring (1.b) and spatial blurring (1.c) categories. The improved performance of BCS can be attributed to its the spatially varying non-local averaging feature and its ability to adapt to the cardiac and respiratory patterns of the specific subject. A high inter-observer variability is seen for aliasing artifacts category. This is expected since all the imaging methods are relatively new to the radiologists. Fig. 1 shows a single frame and a time profile of few slices from one subject for all the methods. Qualitatively we see significant diaphragm border blurring as pointed out by arrows in these images. From the lung volume changes and segmentation contours shown in Fig. 2, we observe that BCS has improved temporal fidelity as compared to other schemes, which suffer from significant temporal blurring. Fig. 3 shows the change in lung volume and segmented lung for the same subject with two maneuvers. The normal minute ventilation was found to be 4L/min and the supine inspiratory capacity in deep breathing maneuver was 1.5L, which correlates well with the literature for normal subjects in the supine position.

Conclusion:

Our study indicates that the BCS scheme gives individualized reconstructions with diagnostically useful image quality and minimal spatio-temporal blurring compared to other accelerated imaging schemes.

Acknowledgements

No acknowledgement found.

References

1. Gierada DS, Curtin JJ, Erickson SJ et al. Diaphragmatic motion: fast gradient-recalled-echo MR imaging in healthy subjects. *Radiology* 194(3), 879-884 (1995).
2. Craighero S, Promayon E, Baconnier P et al. Dynamic echo-planar MR imaging of the diaphragm for a 3D dynamic analysis. *European radiology* 15(4), 742-748 (2005).
3. Bhave S, Lingala SG, Johnson CP et al. Accelerated whole-brain multi-parameter mapping using blind compressed sensing. *Magnetic Resonance in Medicine* (2015).
4. Lingala SG & Jacob M. Blind compressive sensing dynamic MRI. *IEEE Transactions on Medical Imaging*, 32(6), 1132-1145 (2013).

Figures



Figure 1: The figure shows comparison between view sharing, nuclear norm minimization, l_1 Fourier sparsity regularization and BCS scheme (Rows 1-4) for 4 of the 16 slices on subject 1. It is seen that BCS provides superior spatio-temporal fidelity in comparison to the other methods (see yellow arrows).

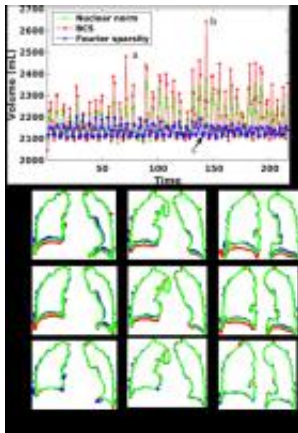


Figure 2: The plot shows the volume of lung as a function of time. The second, third and fourth rows show the lung segmentation contours for the three methods at three time points. From the plot and segmentations, we see that both methods except BCS suffer from considerable temporal blurring.

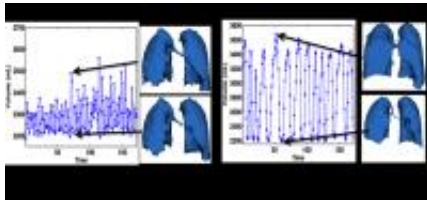


Figure 3: The figure shows the changes in lung volumes for tidal breathing (left) and deep breathing (right) maneuver. The segmented lung volumes during peak inhalation and exhalation are also shown. The normal minute ventilation for supine position was around 4L/min. The supine inspiratory capacity was measured to be 1.5L.

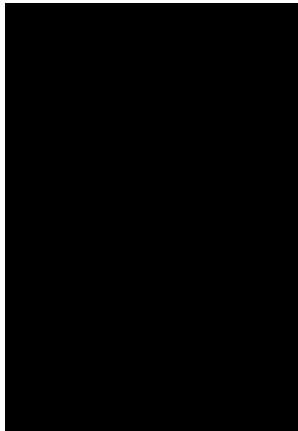


Table 1: Clinical Scores by two radiologists: We observe that all methods except view sharing are comparable in terms of minimizing aliasing artifacts as seen in 1.a. BCS has minimal spatio-temporal blurring as compared to other methods as indicated by higher scores in temporal and spatial blurring categories (1. b-c)